Conformational Heterogeneity of Tryptophan in a Protein Crystal

Tanya E. S. Dahms,[‡,†] Kevin J. Willis,[§] and Arthur G. Szabo*[,‡,⊥]

Contribution from the Department of Chemistry and Biochemistry, University of Windsor, Windsor, Ontario N9B 3P4, Canada, Department of Biochemistry, University of Ottawa, Ottawa, Ontario K1H 8M5, Canada, and Institute for Biological Sciences, National Research Council of Canada, M-54 Montreal Road, Ottawa, Ontario K1A 0R6, Canada

Received July 13, 1994[⊗]

Abstract: Time-resolved fluorescence decay measurements of individual erabutoxin *b* protein crystals showed evidence of conformational heterogeneity for the single tryptophan residue, Trp 29. The relative proportion of each decay component was dependent on the angular orientation of the crystal with respect to the polarization of the incident excitation laser beam. The experimental data demonstrate the existence of rotamers of the tryptophan residue side chain in the protein crystal. Model functions which simulate the orientational dependence of the decay component relative proportions were consistent with this rationalization. These results confirm the "rotamer" model for the interpretation of tryptophan fluorescence decay of proteins in solution.

Introduction

The spectroscopic study of proteins has provided new insights into the relationships between their structure, dynamics, and function. The fluorescence properties of tryptophan (Trp) allow for the elucidation of local structural features and segmental dynamics. In many cases this is sufficient for an improved understanding of the overall molecular details of structure−function correlations. Increasingly, single Trp mutants of selected proteins, where the Trp residue may be site specifically incorporated into different segments of the protein, have been investigated by time-resolved fluorescence methods.[1−3] Single Trp-containing proteins have often been shown to exhibit multiexponential fluorescence decay kinetics in aqueous solution.[4,5] This observation has been rationalized in terms of the conformational heterogeneity of the Trp residue originating from different rotamer conformations.[6,7] The "rotamer" model proposes that the Trp side chain may adopt low-energy conformations, due to rotation about the Cα−Cβ and/or the Cβ−Cγ bonds of the side chain,[8] with each conformation displaying a distinct decay time. This model originated from studies on Trp in a diketopiperazine[9] and Trp zwitterion[10,11] and was shown to be applicable to fluorescence decay studies of small peptides, where the relative proportions of each decay component corresponded to the individual rotamer populations measured by NMR.[6] Recently, it has been suggested that the relative proportions of the fluorescence decay components may be correlated with localized protein secondary structure via its influence on rotamer populations.[7]

For protein crystals, the electron density of the Trp side chain (when compared with other residues) is considered to be "well-defined" by crystallographic criteria and is almost exclusively modeled as a single conformer. Therefore, one might expect that single-exponential decay kinetics would be observed for an individual tryptophan residue in a crystalline protein. In this case, measuring the fluorescence parameters of single protein crystals could provide a direct comparison between a particular fluorescence lifetime and local structural features of the Trp environment (defined by the X-ray crystal structure). This would provide a better understanding of the factors governing Trp fluorescence in solution leading to an enhanced information content of protein fluorescence parameters.

Time-resolved fluorescence studies of the crystalline heme protein myoglobin[12] have demonstrated the feasibility of accurately measuring Trp fluorescence decay parameters from protein crystals. In the case of myoglobin, the fluorescence decay times of the Trp residues were primarily determined by the rate of energy transfer from Trp to the heme group. Since this rate of deactivation greatly exceeds that of all other competing processes, information on local structural details of the protein from Trp fluorescence was not observable.

Erabutoxin *b* (3EBX) contains a single Trp residue (Trp 29) which is invariant in snake neurotoxins and has been shown to be important in interactions with the acetylcholine receptor.[13] The crystal structure of 3EBX has been determined[14,15] and refined to 1.4 Å resolution[16] with the Trp residue modeled in a single conformation ($\chi_1 = 72.8$, $\chi_2 = -88.7$).[17] The present

‡ University of Ottawa.
† National Research Council.
⊥ Address correspondence to this author at the University of Windsor.
§ Current address: Procept Inc., 840 Memorial Dr., Cambridge, MA 02139.
⊗ Abstract published in *Advance ACS Abstracts*, February 1, 1995.

(1) Harris, D. L.; Hudson, B. S. *Biochemistry* **1990**, *29*, 5276−5285.
(2) Hutnik, C. M. L.; MacManus, J. P.; Banville, D.; Szabo, A. G. *Biochemistry* **1991**, *30*, 7652−7660.
(3) Kilhofer, M. C.; Kubina, M.; Travers, F.; Haiech, J. *Biochemistry* **1992**, *31*, 8098−8106.
(4) Beechem, J. M.; Brand, L. *Annu. Rev. Biochem.* **1985**, *54*, 43−71.
(5) Eftink, M. *Methods of Biochemical Analysis: Protein Structure Determination*; Suelter, C. H., Ed.; John Wiley: New York, 1991; Vol. 35, pp 129−207.
(6) Ross, J. B. A.; Wyssbrod, H. R.; Porter, R. A.; Schwartz, G. P.; Michaels, C. A.; Laws, W. R. *Biochemistry* **1992**, *31*, 1585−1594.
(7) Willis, K. J.; Szabo, A. G. *Biochemistry* **1992**, *31*, 8924−8931.
(8) Gordon, H. L.; Jarrell, H. C.; Szabo, A. G.; Willis, K. J.; Somorjai, R. L. *J. Phys. Chem.* **1992**, *96*, 1915−1921.
(9) Donzel, B.; Gauduchon, P.; Wahl, Ph. *J. Am. Chem. Soc.* **1974**, *96*, 801−808.
(10) Szabo A. G.; Rayner, D. M. *J. Am. Chem. Soc.* **1980**, *102*, 554−563.
(11) Chang, M. C.; Petrich, J. W.; MacDonald, D. B.; Fleming, G. R. *J. Am. Chem. Soc.* **1983**, *105*, 3819−3832.
(12) Willis, K. J.; Szabo, A. G.; Krajcarski, D. T. *J. Am. Chem. Soc.* **1991**, *113*, 2000−2002.
(13) Chang, C. C.; Yang, C. C. *Biochim. Biophys. Acta* **1973**, *295*, 595−604.
(14) Tsernoglou, D.; Petsko, G. A. *FEBS Lett.* **1976**, *68*, 1−4.
(15) Low, B. W.; Preston, H. S.; Sato, A.; Rosen, L. S.; Searl, J. E.; Rudko, A. D.; Richardson, J. S. *Proc. Natl. Acad. Sci. U.S.A*, **1976**, *73*, 2991−2994.

0002-7863/95/1517-2321$09.00/0

study investigates the steady-state and time-resolved fluorescence parameters of the Trp residue in single 3EBX crystals as well as in solution.

Experimental Section

Protein Preparation. Erabutoxin *b* was purchased from Sigma Chemical Co. (Lot No. 20H4046) and was further purified by weak cation exchange HPLC on a TSK CM-5PW column with 0.01 M sodium acetate pH 6.5 using a sodium chloride (NaCl) gradient (3EBX eluted at ~0.029 M NaCl). Electro-spray ionization (ESI) mass spectrometry (API III quadrupole. Sciex, Mississauga, Ontario, Canada) was used to verify protein identity and purity. Crystals (0.2 mm × 0.05 mm) of 3EBX were grown by the hanging droplet method using commercial protein dissolved in deionized water (~26 mg/mL) mixed 1:1 with 35−37% (v/v) saturated ammonium sulfate, similar to published procedures.[14]

Fluorescence Measurements. Single crystals, washed with protein-free mother liquor, were placed centrally on the inside front face of a round cell (width = 2 mm, diameter = 2 cm) containing 50 μL of protein-free mother liquor to provide solvent humidity. The cell was sealed with parafilm and mounted on a device consisting of a goniometer attached to an *x,y,z* translation stage, such that the front face of the cell was perpendicular to the goniometer rotational axis.

Steady-State Fluorescence. Steady-state fluorescence measurements of 3EBX crystals were made on the time-resolved instrument in the following manner: The fluorescence intensity, at a series of emission wavelengths, was determined by integration of the fluorescence decay curve over a fixed time period and subsequently corrected for instrument response using *N*-acetyltryptophanamide as a fluorescence standard.

Time-Resolved Fluorescence. Detailed procedures and instrumentation used for time-resolved and steady-state fluorescence measurements have been described elsewhere.[18] These measurements were performed using time-correlated single-photon counting with laser/microchannel plate based instrumentation. The unfocussed, vertically polarized excitation beam (295 nm, diameter ~ 0.75 mm) was incident on the cell at an angle of 35° to the normal of the cell face. This prevented specularly reflected light from entering the "right angle geometry" detection optics.[19] Prior to detection, the emitted light passed through a polarizer oriented 55° to the vertical, a glass filter (3 mm path length), and a JY H10 monochrometer with a 4 nm band pass. The filter transmittance was 0.002% at 295 nm and ~29% at 326 nm. The data were collected in 2048 channels at 10 ps/channel in a multichannel analyzer. The instrument response function was determined from the Raman scattering of the excitation beam by water[20] in an identical cell at 326 nm (fwhm typically 50 ps). For protein samples in solution, corrections were made for the very weak signal from the protein-free blank. Simultaneous (global) analysis of multiple time-resolved data sets has been described elsewhere.[18,21] The best fit between the experimentally measured decay curve and the mathematically convolved curve is determined by a minimization of the weighted sum of squares of the differences (residuals) between the experimental and calculated points. The statistical criteria SVR and σ are based upon the determination of the weighted residuals and were used to assess the adequacy of the data analysis.[22] The σ value (acceptable fit between 1.1and 1.0) is defined as the square root of the reduced χ^2 and the SVR (acceptable fit between 1.7 and 2.0) is able to provide a measure of the correlation between successive residuals.

Orientation Experiments. Orientation experiments were performed by rotating the crystal with respect to the plane of excitation polarization and the fluorescence decay behavior was measured at 10° rotation intervals. After several data sets were collected for the same crystal, the sample was returned to the original orientation and the fluorescence decay parameters were remeasured in order to assess crystal photodamage. If the parameters were different from those originally measured, then the data sets obtained between the previous reproducible data set and the non-reproducible data set were discarded.

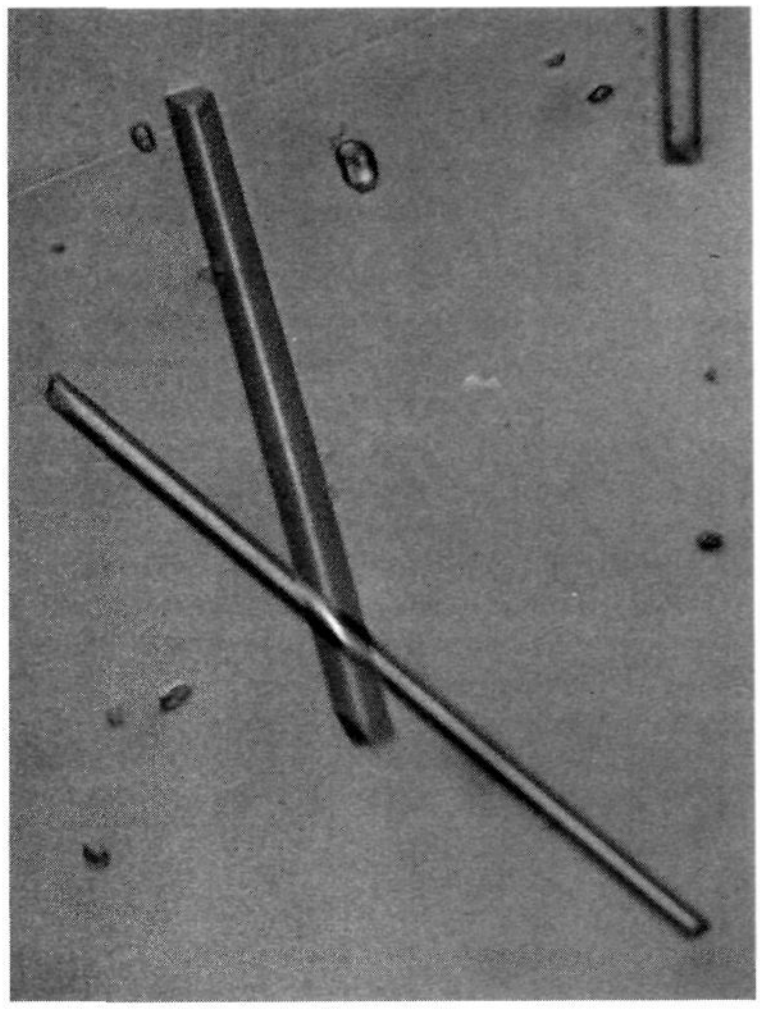

Figure 1. Microphotograph of erabutoxin *b* protein crystals (longest dimension ≈ 0.2 mm).

Results

Protein Preparation. Erabutoxin *b*, which was crystallized using conditions similar to those previously published,[14] produced rod-shaped crystals (Figure 1) that were >99% pure by HPLC. The molecular weight of the HPLC purified protein as well as that of the crystalline material was determined by ESI mass spectrometry (6860.1; calculated 6860.8). The crystals produced a diffraction pattern, however full determination of the crystallographic cell parameters was impeded by the small crystal size (0.2 mm × 0.05 mm).

Fluorescence Measurements. The excitation of Trp 29 from single 3EBX crystals with 295 nm light from the laser system produced a significant fluorescence signal. The photon count rate was dependent upon crystal size and orientation. When there was a decrease in count rate of greater than 15% during excitation, crystal photodamage was observed as evidence by cracking of the crystal (observed under a microscope).

The steady state spectrum of the 3EBX crystals was identical with that in aqueous buffer, having an emission maximum at 340 nm (Figure 2).

Time-resolved fluorescence decay measurements of 3EBX in buffered solution at 12 individual emission wavelengths (305−400 nm) displayed three exponential decay components whose decay times were similar at each wavelength. This justified the global analysis of these data sets to provide the decay times displayed in Table 1. It is possible to obtain a decay-associated spectra (DAS) by combining the steady state and time-resolved fluorescence data (Figure 2). The intermediate decay component (1.17 ns) makes the largest relative contribution (85%) to the fluorescence spectra, whereas the longest (3.64 ns) and shortest (0.28 ns) decay components each

(16) Smith, J. L.; Corfield, P. W. R.; Hendrickson, W. A.; Low, B. *Acta Crystallogr.* **1988**, *A44*, 357−368.
(17) Bernstein, F. C.; Koetzle, T. F.; Williams, G. J. B.; Meyer, E. F., Jr; Brice, M. D.; Rodgers, J. R.; Kennard, O.; Shimanouchi, T.; Tasumi, M. *J. Mol. Biol.* **1977**, *112*, 535−542.
(18) Willis, K. J.; Szabo, A. G. *Biochemistry* **1989**, *28*, 4902−4908.
(19) Eisinger, J.; Flores, J. *J. Anal. Biochem.* **1979**, *94*, 15−21.
(20) Willis, K. J.; Szabo, A. G.; Krajcarski, D. T. *Photochem. Photobiol.* **1990**, *51*, 375−377.
(21) Knutson, J. R.; Beechem, J. M.; Brand, L. *Chem. Phys. Lett.* **1983**, *102*, 501−507.
(22) Durbin, J.; Watson, G. S. *Biometrika* **1971**, *58*, 1−19.
(23) Diamond, R. *Acta Crystallogr.* **1988**, *44*, 211−216.

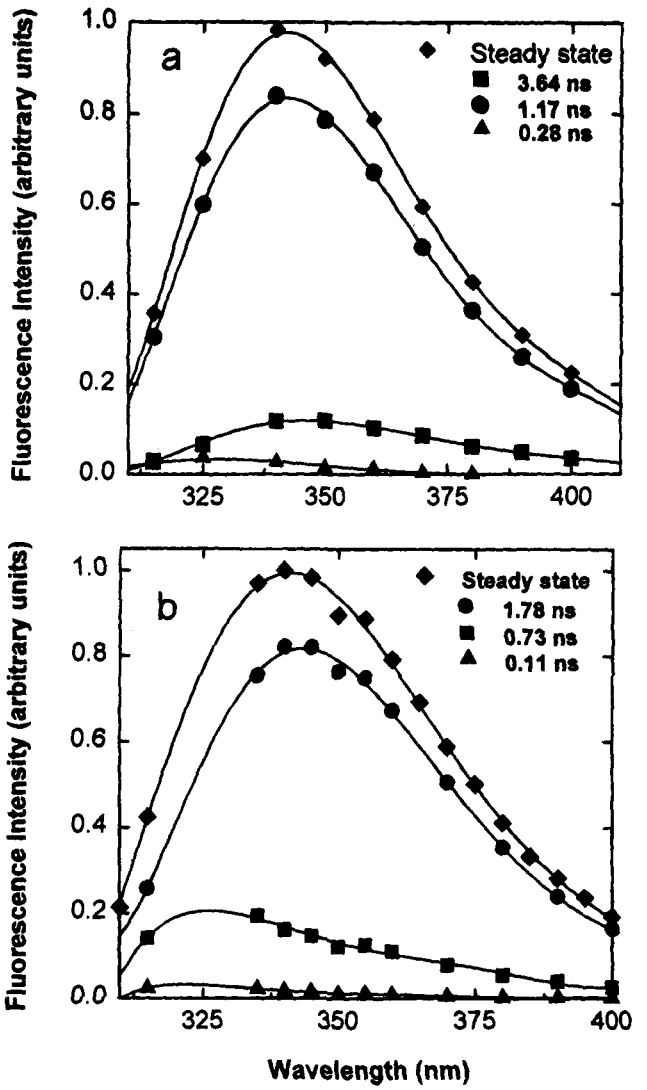

Figure 2. DAS of 3EBX in solution and in the crystalline state. The standard errors and statistics as specified in Table 1 apply. The DAS of 3EBX in the crystalline state was measured at one protein crystal orientation. The shape and relative proportions of each curve are affected by the crystal alignment with respect to the polarized excitation source.

Table 1. Time-Resolved Trp Fluorescence of 3EBX in Solution and in the Crystalline State: Fluorescence Decay Times from the Global Analysis of Multiple Emission Wavelengths (295 nm Excitation, 20 °C, pH 7) As Compared with Literature Values[25]

3EBX	τ_1[a] (ns)	τ_2 (ns)	τ_3 (ns)	$\langle\tau\rangle$	SVR	χ^2 (σ)
solution	3.64	1.171	0.276	1.72	1.81	1.09
crystal	1.78	0.734	0.113	0.55	1.71	1.12
solution (Tanaka)[25]	4.30	1.11		1.80		3.36

[a] The fluorescence lifetime values of 3EBX in solution were generated by the global analysis of a multiple wavelength experiment (12 data sets). The fluorescence lifetimes of the 3EBX crystal were determined by the global analysis of combined data from a multiple (10 data sets) wavelength and a multiple orientation (10 data sets) experiment. Typical errors associated with τ_1, τ_2, τ_3 were ± 0.02, ±0.002, and ±0.004 for 3EBX in solution and ± 0.002, ±0.004, and ±0.002 for 3EBX in the crystalline state.

made a small relative contribution (4% and 12%, respectively). The spectral maximum of the long and intermediate decay components is similar to that of the steady state spectrum, whereas the spectral maximum of the shortest decay time seems to be shifted to a lower wavelength (Figure 2).

Contrary to expectations, the Trp fluorescence of 3EBX single crystals also required three decay times to model the fluorescence decay kinetics (Table 1). Ten crystals were examined, each producing similar fluorescence decay parameters and statistics allowing for the global analysis of these data. However, there is a limit to the total number of data sets which can be simultaneously analyzed precluding the global analysis of the ten sets of data. Global analysis combining several fluorescence decay data sets for three individual crystals produced acceptable statistics, confirming the consistency of the data measured from different crystals. The fluorescence decay times were also obtained from the global analysis of a combination of 20 data sets from measurements made at 10 different emission wavelengths (305−400 nm) and ten angular orientations of a single crystal, exhibiting values and statistics consistent with those previously determined. The longest decay component (1.78 ns) displayed a spectral maximum similar to that of the steady state spectrum whereas the spectral maximum of the two shorter decay components (0.73 ns and 0.11 ns) were shifted to lower wavelengths (Figure 2).

Orientation Experiments. In order to assess the origin of the multiexponential decay behavior of Trp 29 fluorescence in crystalline 3EBX, the crystals were rotated around the excitation laser beam axis of vertical polarization. The fluorescence decay times remained constant at all orientation angles but it was found that the normalized pre-exponential terms varied. The orientational dependence of the normalized pre-exponential terms of each decay component for three different crystals is displayed in Figure 3 (parts a−c). Full 360° rotation experiments were precluded by eventual crystal photodamage. Orientation experiments were performed on several individual crystals and each produced three distinct functions for the normalized pre-exponential terms. In two of the three orientation experiments illustrated, there was a significant orientational dependence of these terms (Figure 3a,b). It was possible to combine 20 data sets, 10 each from two different crystals, in order to confirm the consistency of the lifetime values. When this analysis was performed in all three possible combinations with the lifetime values fixed to the mean values from the global analysis of the three individual crystal data sets (Table 1), satisfactory statistical parameters were obtained (SVR = 1.73 and χ^2 = 1.11).

Discussion

The original objective of this work was to develop an interpretive database for Trp fluorescence from time-resolved studies of single Trp protein crystals. The fluorescence parameters could then be correlated with the structural information for each Trp residue. Examination of the Brookhaven protein data bank[17] revealed that Trp had been almost exclusively modeled as a single conformation in each of the protein crystal structures. Therefore, it was reasonably expected that single exponential fluorescence decay kinetics might be observed for an individual Trp residue in a crystalline protein.

The emission maxima for 3EBX in solution and in the crystalline state are identical (340 nm), indicating that the Trp 29 residue within the protein crystal seems to remain in a very polar environment. This can be accounted for by the many water molecules which have been modeled into the crystal lattice of 3EBX. The Trp of 3EBX is very solvent exposed (as compared with Trp in other proteins) due to the overall flat structure arising from the β-sheet secondary structural motif.

The fluorescence of Trp 29 in 3EBX is best described by triple exponential decay kinetics both in solution and in the crystalline state. The three fluorescence decay times exhibited by the 3EBX crystals are much shorter than those observed in solution (Table 1). Quenching of the Trp fluorescence in the crystal likely results from local intermolecular interactions in the crystalline state which are not present in solution. The most

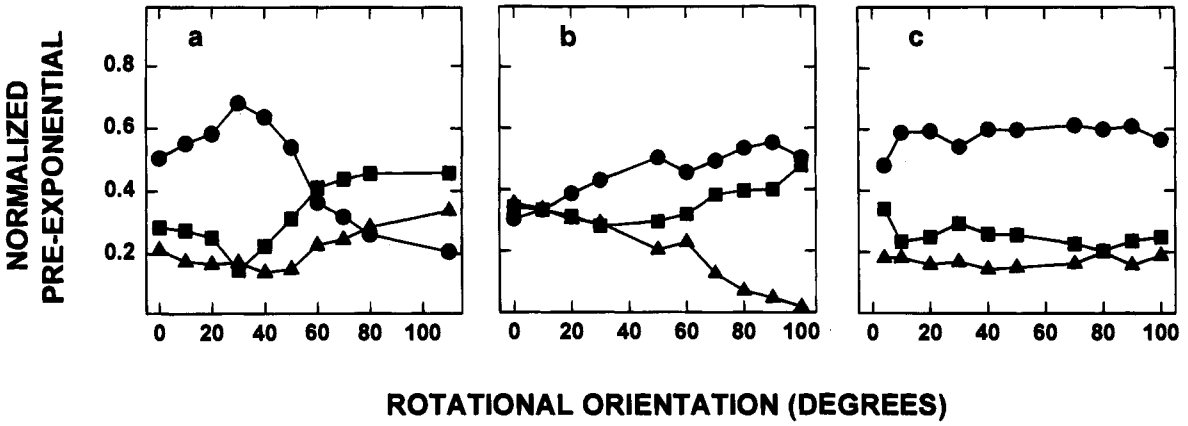

Figure 3. Dependence of the fluorescence decay-time component proportions on crystal orientation with respect to the polarization of the excitation beam. Parts a, b, and c represent data acquired from individual 3EBX protein crystals: (●) 1.78 ns, (■) 0.73 ns, (▲) 0.11 ns.

likely candidate for fluorescence quenching is a disulfide moiety located close to the Trp residue. Examination of the crystal structure[16] showed that the distance from the nearest intramolecular disulfide residue to Trp 29 is 13−14 Å. However, the 3EBX molecules are packed together in the crystal such that the intermolecular distance from the disulfide of one protein molecule and Trp 29 of an adjacent molecule is considerably closer (6.9 Å). Model studies with synthetic cyclic tripeptides which examined the distance dependence of Trp fluorescence quenching by disulfide groups showed that the critical quenching distance is 7 Å.[24] The mechanism of quenching was not apparent from this earlier study, however several common pathways were rejected and it was proposed that a vibrational dissipation of the excitation energy was facilitated via an extremely short-range interaction between the aromatic ring and the sulfur atoms. The average lifetime ($\langle\tau\rangle$) value of 3EBX in solution (1.72 ns) was consistent with the value reported by Tanaka *et al.* (1.80 ns),[25] but the individual fluorescence decay times did not agree with those previously measured (Table 1). This discrepancy may arise from the difficulty of the earlier study to adequately resolve the short decay time, which is evidenced by the large χ^2 value (3.36) reported in that study.

Steady-state and time-resolved data were combined to generate DAS, representing the relative contribution of each decay time component to the total fluorescence as a function of wavelength. The DAS of 3EBX in solution (Figure 2a) reveals that the shortest decay component has a "blue-shifted" spectra, indicating that this emitting species experiences a more hydrophobic environment than the other two rotamers. In the case of the 3EBX crystal, both of the two shorter decay components exhibit maxima at a lower wavelength which is consistent with emission from a highly quenched tryptophan in a nonpolar environment.

Time-resolved data for 3EBX in solution at 300-nm excitation were consistent with that measured at 295-nm (data not shown) with acceptable statistical fits. Therefore, there is no evidence of significant Tyr 25 fluorescence contribution at 295-nm excitation that might otherwise account for a blue-shifted spectra.

The observation of three exponential decay components for the 3EBX crystals is the most significant aspect of this work. There are two possible explanations for this result. The first model consists of the Trp side chain in a single conformation with heterogeneous surrounding residues. Several fluorescence lifetimes would arise due to different quenching mechanisms of at least three distinct local Trp environments conferred by alternate protein or surrounding side chain conformations. The second model proposes conformational heterogeneity of the Trp side chain, with only one of the conformers being detected by X-ray crystallography. In the latter model, the individual Trp residue of each protein molecule within the crystal could adopt at least three distinct conformations. The interaction of the Trp side chain with different structural elements (protein backbone or other side chains) would lead to different fluorescence decay times. There would be no possibility of conformer exchange on the time scale of the fluorescence measurement. The latter interpretation is the basis for the rotamer model of Trp fluorescence decay behavior in protein solutions.

In order to test these two hypotheses, orientation experiments were designed based on the following reasoning: The absorption of the Trp residue depends on the angular orientation of the excited state transition moment with respect to the polarization direction of the excitation beam. Maximum absorption will occur when the transition dipole is aligned with the excitation plane of polarization. At 295 nm the L_a transition of Trp is likely the dominant one, with the L_b transition making only a minor contribution to the absorbance.[26] Therefore, the fluorescence should be primarily from the L_a singlet state. Since the fluorescence intensity is proportional to the square of the absorption transition probability, then the fluorescence intensity of a fluorophore should vary with an angular dependence of the fluorophore's dipole with respect to the polarization direction (vertical) of the excitation source. In this case, there are effectively three fluorophores (one for each rotamer) and the relative intensity of each will be reflected in the normalized pre-exponential terms derived from the fluorescence decay curve. An orientational dependence of the normalized pre-exponential terms for each fluorescence decay should be expected if the rotamer hypothesis were correct, since each rotamer (and therefore each dipole) would be aligned differently in the crystal. If the three fluorescence decay times were the result of three distinct Trp conformers in separate molecules of the crystal, then the relative proportions (normalized pre-exponential terms) of the decay components should vary with crystal orientation but the decay time values should not. If the data were to be explained by the first model where the Trp is in a single conformation with alternate local environments, then no variation of the normalized pre-exponential terms should be observed during the orientation experiments.

Significantly, the normalized pre-exponential terms (which correspond to the relative contributions of each decay compo-

(24) Cowgill, R. W. *Biochim. Biophys. Acta* **1970**, *207*, 556−559.
(25) Tanaka, F.; Kaneda, N.; Mataga, N.; Tamai, N.; Yamazaki, I.; Hayashi, K. *J. Phys. Chem.* **1987**, *91*, 6344−6346.
(26) Valeur, B.; Weber, G. *Photochem. Photobiol.* **1977**, *25*, 441−444.

nent) were dependent on the crystal orientation. This provides direct evidence for at least three Trp side chain rotamer conformations (contained in separate protein molecules) within the crystals. Figures 3a and 3b show two examples of crystals in which there was significant variation of the pre-exponential terms with crystal orientation. Two of the 3EBX crystals for which an orientation experiment was performed exhibited only limited variation of the pre-exponential terms (represented in Figure 3c).

Simulations and Calculations. It was possible to simulate the pattern for the orientational dependence of the normalized pre-exponential terms. These calculations took into account the exact experimental geometry: the four 3EBX molecules in the crystallographic unit cell; different possible populations of each Trp conformer within the protein crystal; and alternate starting positions of the 3EBX crystal in the sample cell.

A program was written to calculate the theoretical dependence of the relative decay-time proportions on protein crystal orientation, in which the other two tryptophan side chain rotamers, not found by X-ray crystallography (simulated using QUANTA), were included and the initial population of each rotamer could be varied. Since the two alternate Trp orientations were unknown, the conformations originally chosen for the simulations were modeled with a χ_1 rotation of exactly 120° from the crystallographically determined rotamer (g^+, g^-, and t Trp rotamers). The researchers recognized that this simple approach may not be realistic given the interactions of the Trp side chain with the rest of the protein molecule. Therefore, the sub-program "conformational search" (QUANTA software, employing CHARMM energy calculations) was run on Trp 29 with 3EBX in the absence of water molecules in order to discover alternate Trp low-energy conformations. The two conformers which were closest to the original χ_1/χ_2 angles were chosen. A χ_1 rotation was used to represent rotation of the Trp about the peptide backbone and a χ_2 rotation of 90° was used to represent a Trp ring flip. These rotamers are not resolved by X-ray crystallographic data[16] and are modeled as additional Trp low-energy conformations. The alternate Trp side chain rotamers were modeled into the structure (QUANTA software) using the following χ_1/χ_2 angles from low-energy models found in the conformational search: conformer 2 = −168.94°/−94.7°, conformer 3 = −36.62°/−88.92°. The coordinates of the Trp L_a transition dipole were determined from the spatial coordinates of the indole ring nitrogen and carbon 4 of the indole ring.

In practice, the crystal lay on its long axis (Figure 1) on the side of the sample cell. Therefore the theoretical position of the crystal in the sample cell was assumed to be the long axis of the unit cell. This was simulated by subjecting the initial tryptophan dipole coordinates to a rotation matrix,[23] such that the directional cosines ((l,m,n) = (0,0,1) and θ_1 = 45°) were defined by the crystal axes. The values produced by the initial manipulation were then rotated through a second matrix (at intervals of 10° for θ_2) in which l,m,n were defined by the exact experimental geometry. Final values were squared (since the fluorescence is proportional to the square of the absorbance) and the relative proportion of each theoretical fluorophore was calculated. Due to the predominant flat face of the crystal long axis (Figure 1), the crystals could be consistently positioned along the length of the rod; however the initial angular position of the crystals with respect to the vertically polarized laser beam could not be achieved with any precision. The protein crystals could not be repositioned due to their fragile nature. The latter affects the experimental observations such that different portions (up to 100°) of the total orientational variations (360°) were sampled with each crystal.

A change in the relative population of each Trp side chain rotamer was found to alter the shape and amplitude of the orientation dependence curves (data not shown). The rotamer which is most predominant could not be absolutely determined from the crystal fluorescence data. The simulation curve which was produced by assuming the relative proportions of the three rotamer populations to be 0.1, 0.2, and 0.7 (values similar to those determined by solution fluorescence) is shown in Figure 4a. There are some remarkable similarities between the experimental curves (Figure 3a,b,c) and portions of the simulated curve (Figure 4a). Part of this simulation (165−195°) shows dramatic variation of the rotamer proportions like the experimental results shown in Figures 3a and 3b. The orientation experiment illustrated in Figure 3c (representative of data from two different crystals) showed only a limited variation of the pre-exponential values and was similar to another portion (140−165°, 195−240°) of the simulation pattern shown in Figure 4A. Experimentally, it was possible to sample only a 100° portion of a total 360° (180° considering periodicity) rotation. It would seem that the portions of the entire curve were sampled randomly according to the initial orientation of the crystal, producing subsets of the entire curve. It could be argued that the minimal orientational dependence shown in Figure 3c is representative of Trp in a single conformation but with alternate environments conferred by other heterogeneous side chains within a critical distance of the Trp. In this case, the crystal would surely exhibit different fluorescence decay times than the other two crystals and this is not the case. An alternative explanation for the minimal variation observed in Figure 3c would be that there are different proportions of the three rotamers in each crystal. However, altering the initial set of rotamer proportions for the simulations produced an entirely distinct set of orientation curves (data not shown). During the simulations, altering the initial orientation of the crystal (x, y, or z axis) upon the sample cell face also produced a distinct set of curves (Figure 3b); however the curves generated using the long axis of the crystal unit cell gave results most representative of the experimental results.

When the two alternate rotamers were modeled with similar χ_2 angles, effectively only changing χ_1 by approximately 120°, the periodicity (~180°) was similar to that found experimentally. On the other hand, when one of the three χ_1 rotamers was modeled with the χ_2 angle 90° from the other two rotamers (Trp ring flip), the periodicity was significantly reduced to less than 60°. This was markedly different from that observed for all

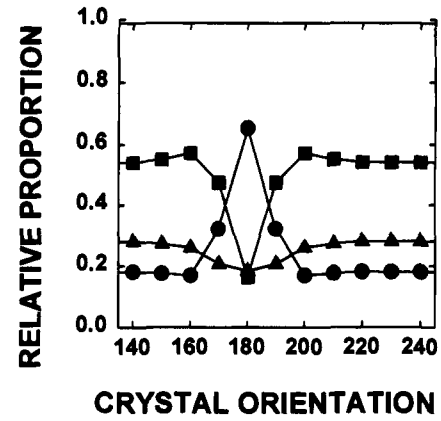

Figure 4. Theoretical orientational dependence (180°) of the relative fluorescence decay-time proportions for 3EBX protein crystals. Simulated data where Trp χ_1 = 72.8°, χ_2 = −88.7°/χ_1 = −168.94°, χ_2 = −94.7°/ χ_1 = −36.62°, χ_2 = −88.9° (g^{+-}, g^{2-}, and t^-, respectively), with 0.7, 0.1, and 0.2 as the relative proportions of the three rotamers and excitation polarization perpendicular to the z-axis of the crystal unit cell.

experimental measurements and provides evidence that the alternate rotamers existing in the crystal may be similar to those modeled in this simulation.

Several recent studies[27,28a,29] have examined side chain rotamer populations in various X-ray crystal structures of proteins (resolution ~ 2.0 Å). These studies show that the mean positions,for $\chi_1 = 60°$, 180°, and −60° (g^+, t, and g^-), based on secondary structural features,[30] are not necessarily accurate representations of many side chain rotamers but can serve as a starting position for predicting side chain conformations in proteins. Factors which seem to affect the "rotamericity" of side chains include backbone torsions of the residue under consideration as well as tertiary packing constraints.[28a,29] The designations of g^{+-}, g^{--} and t^- used herein are the same as those defined by Ponder and Richards, whose rotamer library[27] is a compilation of non-secondary structure-specific rotamer frequencies for all amino acids, based on 19 well-determined crystal structures. The rotamer frequencies found by Ponder and Richards for the rotamers modeled in this study are 20.7% (g^{+-}), 6.9% (g^{--}), and 13.8% (t^-), with only the g^{--} χ_1 value differing significantly from the value used in this study. When normalized, the values are 0.50 (g^{+-}), 0.17 (g^{--}), and 0.33 (t^-), showing a trend which was similar to the relative proportions used in our simulations, namely 0.70 (g^{+-}), 0.10 (g^{--}), and 0.20 (t^-). Based on the ϕ, ψ angles (−161.3° and 171.8°, respectively) defined for Trp 29 in the 3EBX structure, the rotamer library constructed by Schrauber and co-workers[29] would predict a significant population of g^{+-} (21%), g^{--} (4%), and t^- (9%). The normalized values of these three rotamers can be calculated as 0.62, 0.12, and 0.26, respectively, in good agreement with the 0.70, 0.10, and 0.20 values used for our simulation. This rotamer library included a large sample (85 Trp side chains) in the β-strand classification, which is advantageous; however the ϕ, ψ range was large (−240° to 0° and 60° to 230°, respectively). Data from the updated rotamer library constructed by Dunbrack and Karplus[28b] have been sorted into all possible combinations of 20° ϕ, ψ angle increments. Only four Trp residues are found in the ϕ, ψ range defined by the 3EBX crystal structure and these are populated as g^{++} (50%), g^{+-} (25%), and t^- (25%) rotamers. The prediction of three predominant rotamers by the aforementioned studies is consistent with the three rotamers detected in this study. There are significant discrepancies between our simulations and the predictions from two of the three rotamer libraries[28a,29] and none of the libraries predicts three χ_1 rotamers with similar χ_2 angles (~ −90°) as being the most frequent.

It should be noted that for this study the Trp rotamers are proposed to exist in separate molecules within the same protein crystal. Conversely, the Trp rotamer libraries are based on side chain conformations arising from proteins with slightly different ϕ, ψ angles (with the exception of gramicidin (1GMA)[31] and relaxin (6RLX)[32] which each have one or more Trp side chains modeled with one alternate rotamer[17]). The frequency of side chain rotamers from the rotamer libraries may still reflect different rotamer populations within one protein crystal, especially in the case where all possible combinations of 20° ϕ, ψ angle increments were used.[28a] It has been suggested that the detection of alternate rotamers (when less than 33% at 1.4 Å resolution) is beyond the detection limits of current X-ray crystallographic techniques[33] and hence the data base used for the rotamer libraries may be considered to be a first approximation.

The orientation-dependent fluorescence decay experiments for single-protein crystals, combined with the simulations of the orientation dependence of the pre-exponential terms, is consistent with the rotamer model for the interpretation of time-resolved fluorescence parameters in proteins. Given the precise relationship between the Trp rotamer coordinates and the coordinates of the crystal faces, it would be possible to calculate the other rotamer angles. This relationship could be obtained from the crystal cell parameters and time-resolved fluorescence measurements at specific crystal orientations (with respect to the polarized excitation source). Identification of the alternate Trp rotamers may lead to the eventual rationalization of non-radiative deactivation pathways for the excited singlet state of Trp. Other single Trp proteins such as the *Pseudomonas* apoazurins and recombinant rat parvalbumin F102W mutant, in which the Trp residues are buried, are the only proteins to display single exponential fluorescence decay kinetics in solution[34,35] and are more likely to exhibit a single fluorescence decay time in the crystalline state. In each case, a direct comparison could be made between fluorescence decay times and local protein structural features. Such studies would significantly enhance the information content of fluorescence decay measurements since the relative rotamer populations will depend on structural features in the vicinity of the Trp residue.[7,28a,36] This will be particularly useful in fluorescence studies of protein−protein interactions where Trp is involved in the interaction.

The observation of conformational heterogeneity for Trp in a protein crystal, which was previously reported to be in a single side chain configuration, has important implications for protein X-ray crystallographic studies. It suggests that a reexamination of the X-ray data for evidence of Trp side chain rotamers is warranted. There are only two protein crystal structures in the Brookhaven data bank exhibiting two separate conformations of the Trp side chain and both these structures are highly resolved (0.86 Å for 1GMA[17,31] and 1.5 Å for 6RLX[17,32]). Perhaps as more and more protein crystal structures are determined to higher resolution, modeling of alternate Trp side chain rotamers will become more frequent. Identification of conformational heterogeneity by very sensitive time-resolved fluorescence techniques and other methods may provide improved levels of structural detail and lead to new insights into the structure−function relationships of proteins.

Acknowledgment. This work was supported in part by a grant from the Natural Science and Engineering Research Council of Canada. The authors thank Mr. D. T. Krajcarski for his expert technical assistance, Dr. R. Campbell for helpful discussion and assistance with the orientational modeling, Dr. M. Yaguchi for the mass spectral measurements, and Mr. Y. Leveille for the construction of the cell holder. Thanks are also given to Dr. R. Dunbrack for preprint information and helpful communications.

JA942268U

(27) Ponders, J. W.; Richards, F. M. *J. Mol. Biol.* **1987**, *193*, 775−791.
(28) (a) Dunbrack, R. L., Jr; Karplus, M. *J. Mol. Biol.* **1993**, *230*, 543−574. (b) Dunbrack, R. L. Personal communication.
(29) Schrauber, H.; Eisenhaber, F.; Argos, P. *J. Mol. Biol.* **1993**, *230*, 592−612.
(30) Janin, J.; Wodak, S.; Levitt, M.; Maigret, B. *J. Mol. Biol.* **1978**, *125*, 357−386.
(31) Langs, D. A. *Science* **1988**, *241*, 188−191.
(32) Eigenbrot, C.; Randal, M.; Quan, C.; Burnier, J.; O'Connell, L.; Rinderknecht, E.; Kossiakoff, A. A. *J. Mol. Biol.* **1991**, *221*, 15−21.
(33) Smith, J. L.; Hendrickson, W. A.; Honzatko, R. B.; Sheriff, S. *Biochemistry* **1986**, *25*, 5018−5027.
(34) Hutnik, C. M. L.; Szabo, A. G. *Biochemistry* **1989**, *28*, 3935−3939.
(35) Pauls, T. L.; Durussel, I.; Cox, J. A.; Clark, I. D.; Szabo, A. G.; Gagné, S. M.; Sykes, B. D.; Berchtold, M. W. *J. Biol. Chem.* **1993**, *268*, 20897−20903.
(36) Dahms, T. E. S.; Szabo, A. G. *Biophys. J.* **1994**, *66*, A66.